

Surface-Specific Interaction of the Extracellular Domain of Protein L1 with Nitrilotriacetic Acid-Terminated Self-Assembled Monolayers

Jörg Fick,[†] Tobias Wolfram,[‡] Ferdinand Belz,[§] and Sylvie Roke*[†][†]*Spectroscopy at Bio-Interfaces, Max-Planck Institute for Metals Research, 70569 Stuttgart, Germany,*[‡]*Biomedical Applications of Engineered Interfaces, and* [§]*Department of New Materials and Biosystems*

Received June 29, 2009. Revised Manuscript Received September 18, 2009

We report a study on the interaction of the extracellular domain of trans-membrane proteins *N*-cadherin and L1 with nitrilotriacetic acid (NTA)-terminated self-assembled monolayers (SAMs) grown on silver and gold surfaces. Quartz crystal microbalance (QCM) and reflection absorption infrared spectroscopy (RAIRS) measurements reveal that upon addition of protein to an NTA-SAM there is a subsequent change in the mass and average chemical structure inside the films formed on the metal substrates. By using vibrational sum frequency generation (VSFG) spectroscopy and making a comparison to SAMs prepared with *n*-alkanethiols, we find that the formed NTA-SAMs are terminated by ethanol molecules from solution. The ethanol signature vanishes after the addition of L1, which indicates that the L1 proteins can interact specifically with the NTA complex. Although the RAIRS spectra display signatures in the amide and fingerprint regions, the VSFG spectra display only a weak feature at 866 cm⁻¹, which possibly indicates that some of the abundant phenyl rings in the complex are ordered. Although cell biology experiments suggest the directional complexation of L1, the VSFG experiments suggest that the α -helices and β -sheets of L1 lack any preferential ordering.

Introduction

Smart cell sensors^{1,2} and clever implants^{3–5} are promising tools for the future. To make such devices, it is necessary to understand the molecular structure and function of a wide variety of lipids, proteins, peptides, and biopolymers and their interactions with suitable materials (metals and biopolymers) that can be used as binding substrates.

Of special interest for cellular applications are cell adhesion proteins L1 and *N*-cadherin. L1 is a member of the immunoglobulin super family (IgSF). Members of this family are thought to be crucial in a variety of processes during the formation of the nervous system such as cell adhesion, cell migration, cell differentiation, neurite formation, and regeneration. Both proteins are known to interact mainly by homophilic interactions with proteins from other cell membranes. This is schematically indicated in Figure 1. Like all proteins, L1 and *N*-cadherin have an N-terminus (amine group) on one side and a C-terminus (carboxylic group) on the other side. The underlying model (see Figure 1a) is that the proteins insert into the cell membrane so that the C-terminus is located inside the cell and the N-terminus is located in the extracellular domain. Cell–cell interaction is facilitated by specific interactions between the extracellular domains of identical proteins that are both inserted in an oriented manner into adjacent cells.^{6,7}

To mimic this cell recognition behavior, the extracellular domains of the proteins are modified by transfecting a mammalian cell line with a plasmid vector that leads to the expression of the recombinant protein, which results in the excretion of the complete extracellular domain of L1 or *N*-cadherin⁸ that is linked

to a histidine tag (on the position indicated by the arrow in Figure 1a). The resulting extracellular domain of L1 or *N*-cadherin can now be linked via a Ni²⁺ complex to a surface⁹ that is prepared with a self-assembled monolayer (SAM) of nitrilotriacetic acid (NTA).^{10–12} This procedure (see Figure 1b) preserves the required directionality for the attachment of the proteins to the surface. The third panel shows that surfaces prepared in such a way indeed express biological activity. The microscopy image shows that C2C12 myoblasts adhere specifically to a surface functionalized with NTA linkers and *N*-cadherin. The right part of the image displays a part of the substrate that has been passivated with polyethylene glycol.¹³ On this part of the substrate, there is no cell binding. Further cell experiments indicate that protein-intermediated cell adhesion indeed requires directionally immobilized protein and that this directionality is maintained when His-tagged proteins interact with NTA functionalized surfaces.⁸ Thus, the cell experiment of Figure 1c and other experiments in the literature (refs 8 and 9 and references therein) indicated that the protein–surface interaction might be directional and site-specific. It would therefore be of interest to explore the possibility of obtaining molecular details of this interaction using surface-specific methods (even though the complete molecular structures of L1 and *N*-cadherin have not been investigated by X-ray diffraction (XRD) because of their inability to crystallize)^{14,15}.

(9) Wolfram, T.; Belz, F.; Schön, T.; Spatz, J. P. *Biointerphases* **2007**, *2*, 44–48.(10) Kroger, D.; Liley, M.; Schiweck, W.; Skerra, A.; Vogel, H. *Biosens. Bioelectron.* **1999**, *14*, 155–161.(11) Du Roure, C.; Debieuvre-Chouvy, O.; Malthete, J.; Silberzan, P. *Langmuir* **2003**, *19*, 14138–1443.(12) Love, J. C.; Estroff, L. A.; Kriebel, J. K.; Nuzzo, R. G.; Whitesides, G. M. *Chem. Rev.* **2005**, *105*, 1103–1170.(13) Blummel, J.; Perschmann, N.; Aydin, D.; Drinjakovic, J.; Surrey, T.; Lopez-Garcia, M.; Kessler, H.; Spatz, J. P. *Biomaterials* **2007**, *28*, 4739–4747.(14) Koch, A. W.; Bozic, D.; Pertz, O.; Engelt, J. *Curr. Opin. Struct. Biol.* **1999**, *9*, 275–281.(15) Kulahin, N.; Kasper, C.; Kristensen, O.; Kastrop, J. S.; Berezin, V.; Bocka, E.; Gajhede, M. *Acta Crystallogr.* **2005**, *F61*, 858–860.

*Corresponding author. E-mail: roke@mf.mpg.de. Fax: +49-711-6893612.

(1) Ratner, B. D. *J. Mol. Recognit.* **1996**, *9*, 617–625.(2) Göpel, W. *Biosens. Bioelectron.* **1998**, *13*, 723–728.(3) Tang, L.; Eaton, J. W. *Am. J. Clin. Pathol.* **1995**, *103*, 466–471.(4) Elbert, D. L.; Hubbell, J. A. *Annu. Rev. Mater. Sci.* **1996**, *26*, 365–394.(5) Wisniewski, N.; Reichert, M. *Colloids Surf., B* **2000**, *18*, 197–219.(6) Schurmann, G.; Haspel, J.; Grumet, M.; Erickson, H. P. *Mol. Biol. Cell* **2001**, *12*, 1765–1773.(7) Halbleib, J. M.; Nelson, W. J. *Genes Dev.* **2006**, *20*, 3199–3241.(8) Wolfram, T.; Spatz, J. P.; Burgess, R. W. *BMC Cell Biol.* **2008**, *9*, 64.

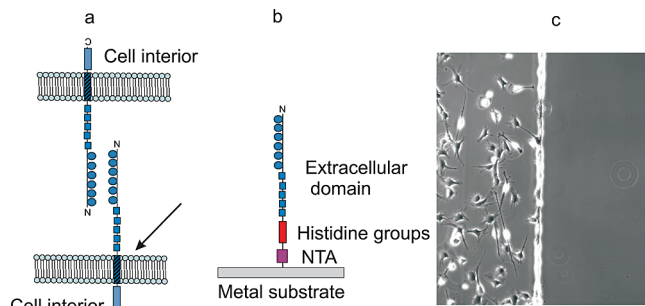


Figure 1. Model of cell–cell interaction mediated by the extracellular domains of proteins. (a) Schematic picture of the protein interaction that facilitates cell–cell adhesion. (b) Illustration of the extracellular protein domain on a functionalized surface. (c) Phase-contrast microscopy image of C2C12 myoblasts on 160 nm spaced gold dots on a glass substrate functionalized with NTA–*N*-cadherin. On the right side of the image, the glass substrate was passivated with poly(ethylene glycol)¹³ so that no cell expression was observed.

Here, we investigate the binding of the complete extracellular domains of L1 and *N*-cadherin to gold and silver surfaces functionalized with NTA-terminated self-assembled monolayers via quartz-crystal microbalance (QCM), reflection absorption infrared spectroscopy (RAIRS), and vibrational sum frequency generation. In a QCM measurement,^{16,17} protein mass adsorption can be followed by monitoring the frequency change of a gold-coated quartz crystal that is electrically kept at resonance. With RAIRS,¹⁸ the collective ensemble of adsorbed vibrational modes can be measured. VSFG is a second-order nonlinear optical technique with which a combined IR and Raman spectrum of a surface is recorded. Because Raman and IR transition moments are allowed simultaneously only at places where inversion symmetry is absent, the method is very interface-specific and sensitive to molecular density, directionality, and order (see, for example, refs 19–23). Recent measurements showed the feasibility of VSFG to help clarify the structure of biologically relevant interfaces containing biopolymers (such as DNA), phospho-

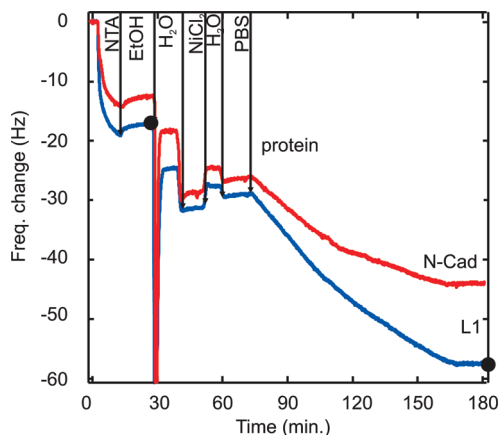


Figure 2. QCM data showing the sequential NTA-mediated binding process of *N*-cadherin (upper trace) and L1 (lower trace) on Au(111) surfaces. At $t = 0$, NTA solution is added to the sample. It can be seen that *N*-cadherin binding is less efficient than L1 binding. The black markers indicate the stages at which the RAIRS and VSFG spectra were taken. The films at these stages are indicated as NTA and NTA–L1 films, respectively.

lipids, and proteins.^{24–36} Obtaining information about the shape and tertiary structure of peptides and proteins adsorbed to silica surfaces,³⁷ angular distributions of the protein with respect to the interface,^{32,38} and probing of the secondary structure have been shown to be possible.³⁹ The combination of QCM and VSFG has been used before,⁴⁰ and in combination with RAIRS, it allows us to determine changes in the mass adsorbed to the surface, changes in the average chemical composition, and changes in the structural organization. It would be very interesting if the directionality suggested by biological experiments could be linked to a clear VSFG signature of the protein.

We find that both *N*-cadherin and L1 can successfully be linked to the surface using an NTA-SAM. The amount of adsorbed mass from the QCM data indicates that the binding of L1 is more efficient, however. Further spectroscopic investigation into L1 binding reveals that ethanol molecules from the aqueous solution play a crucial role in the binding process. In contrast to what is suggested by the biological cell experiments, there is no evidence of any preferential ordering on the surface under atmospheric conditions.

Results and Discussion

In the following section, we describe the QCM results of the interaction of L1 and *N*-cadherin with NTA-SAMs on Au(111). RAIRS and VSFG experiments were performed on both Au(111) and Ag(111) substrates. The data presented here were taken on Ag(111) substrates. The same spectral features were also observed on the Au(111) substrates.

QCM Analysis. Figure 2 represents the QCM data of successive NTA and protein adsorption on Au(111) substrates of *N*-cadherin (upper trace) and L1 (lower trace). It can be seen (in both traces) that the NTA thiol binds to the surface, which is observed through a decrease in the resonance frequency¹⁶ of

(16) Rodahl, M.; Höök, F.; Krozer, A.; Brezinski, P.; Kasemo, B. *Rev. Sci. Instrum.* **1995**, *66*, 3924–3930.

(17) Höök, F.; Rodahl, M.; Kasemo, B.; Brezinski, P. *Proc. Natl. Acad. Sci. U.S.A.* **1998**, *95*, 12271–12276.

(18) Kudelski, A. *Vib. Spectrosc.* **2005**, *39*, 200–213.

(19) Shen, Y. R. *The Principles of Nonlinear Optics*; Wiley: New York, 1984.

(20) Shen, Y. R. *Surf. Sci.* **1994**, *299/300*, 551–562.

(21) Eisenthal, K. B. *Chem. Rev.* **1996**, *96*, 1343–1360.

(22) Bain, C. D. *J. Chem. Soc., Faraday Trans.* **1995**, *91*, 1281–1296.

(23) Chen, X. Y.; Clarke, M. L.; Wang, J.; Chen, Z. *Int. J. Mod. Phys.* **2005**, *19*, 691–713.

(24) Roke, S.; Schins, J. M.; Müller, M.; Bonn, M. *Phys. Rev. Lett.* **2003**, *90*, 128101.

(25) Oh-e, M.; Yokoyama, H.; Yorozuya, S.; Akagi, K.; Belkin, M. A.; Shen, Y. R. *Phys. Rev. Lett.* **2004**, *93*, 267402.

(26) Liu, J.; Conboy, J. C. *J. Am. Chem. Soc.* **2004**, *126*, 8376–8377.

(27) Dreesen, L.; Sartenaer, Y.; Humbert, C.; Mani, A. A.; Lemaire, J. J.; Methivier, C.; Pradier, C. M.; Thiry, P. A.; Peremans, A. *Thin Solid Films* **2004**, *464–65*, 373–378.

(28) Dreesen, L.; Sartenaer, Y.; Humbert, C.; Mani, A. A.; Methivier, C.; Pradier, C. M.; Thiry, P. A.; Peremans, A. *ChemPhysChem* **2004**, *5*, 1719–1725.

(29) Chen, X. Y.; Tang, H. Z.; Even, M. A.; Wang, J.; Tew, G. N.; Chen, Z. *J. Am. Chem. Soc.* **2006**, *128*, 2711–2714.

(30) Ma, G.; Allen, H. C. *Langmuir* **2007**, *23*, 589–597.

(31) Chen, X. Y.; Wang, J.; Paszti, Z.; Wang, F. L.; Schrauben, J. N.; Tarabara, V. V.; Schmaier, A. H.; Chen, Z. *Anal. Bioanal. Chem.* **2007**, *388*, 65–72.

(32) Chen, X. Y.; Wang, J.; Boughton, A. P.; Kristalyn, C. B.; Chen, Z. *J. Am. Chem. Soc.* **2007**, *129*, 1420–1427.

(33) Stokes, G. Y.; Gibbs-Davis, J. M.; Boman, F. C.; Stepp, B. R.; Condie, A. G.; Nguyen, S. T.; Geiger, F. M. *J. Am. Chem. Soc.* **2007**, *129*, 7492–7493.

(34) Sartenaer, Y.; Tourillon, G.; Dreesen, L.; Lis, D.; Mani, A. A.; Thiry, P. A.; Peremans, A. *Biosens. Bioelectron.* **2007**, *22*, 2179–2183.

(35) Sugiharto, A. B.; Johnson, C. M.; Dunlop, I. E.; Roke, S. *J. Phys. Chem. C* **2008**, *112*, 7531–7534.

(36) Howell, C.; Diesner, M. O.; Grunze, M.; Koelsch, P. *Langmuir* **2008**, *24*, 13819–13821.

(37) Kim, J.; Somorjai, G. A. *J. Am. Chem. Soc.* **2003**, *125*, 3150–3158.

(38) Wang, J.; Lee, S. H.; Chen, Z. *J. Phys. Chem. B* **2008**, *112*, 2281–2290.

(39) Chen, X. Y.; Wang, J.; Sniadecki, J. J.; Even, M. A.; Chen, Z. *Langmuir* **2005**, *21*, 2662–2664.

(40) Phillips, D. C.; York, R. L.; Mermut, O.; McCrea, K. R.; Ward, R. S.; Somorjai, G. A. *J. Phys. Chem. C* **2007**, *111*, 255–261.

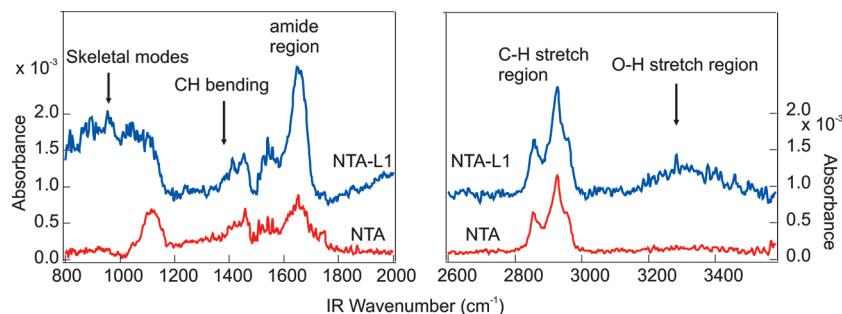


Figure 3. RAIRS spectra of self-assembled NTA films on Ag(111) (lower trace) and self-assembled NTA films with subsequent binding of the His-tagged extracellular domain of the L1 protein (upper trace).

15 Hz (upper trace) and 20 Hz (lower trace). Subsequently, the addition of ethanol results again in a slight change in resonance frequency.

The reason could be that some of the ethanol binds to the carboxylate groups on NTA and thereby changes the viscosity or the mass of the adsorbed films. Adding water and NiCl_2 results again in a change that indicates that Ni^{2+} complexes with NTA but after adding water and PBS some of those groups disappear again. This is consistent with the relatively weak nature of the interaction. Adding L1 or *N*-cadherin in concentrations needed to achieve biological functionality⁹ results in another shift in the resonance frequency, which means that the proteins do attach to the surface. Specifically, a change of around 17 Hz is observed for *N*-cadherin, in contrast to 28 Hz for L1. This change in frequency is comparable to that observed in earlier studies⁴⁰ and is slightly larger but comparable to the change in frequency for NTA binding. Thus, QCM confirms the deposition of NTA and the proteins, showing a lower adsorption in the case of *N*-cadherin. We therefore focus our attention on the adsorption of L1 in the remaining part of the discussion.

Surface Binding of L1 Studied with RAIRS. Figure 3 shows RAIRS spectra of a Ag(111) surface with NTA and NTA-L1, corresponding to the points of preparation indicated in Figure 2. It can be seen that the NTA-L1 intensity is a bit higher than that of just NTA, indicating that the adsorbed mass has indeed increased. Also, the spectra are different, which shows that the two films have a different average chemical composition. More specifically, the NTA films display resonances in the C-H region at 2852 and 2925 cm^{-1} that coincide with the symmetric stretch mode of the CH_2 groups and a Fermi resonance of the symmetric CH_2 stretching vibration with a bending mode. Also present are a band at 1650 cm^{-1} , a broad band at 1350–1450 cm^{-1} , and a peak at 1109 cm^{-1} , which can be assigned, respectively, to the C=O stretching motion, the C-H bending motion, and C-O-C stretching from the ethylene glycol groups, respectively. (See, for example, ref 41.) The spectrum of the NTA-L1 film displays additional intensity in the region between 3100 and 3600 cm^{-1} and below 1200 cm^{-1} . The band between 3100 and 3600 cm^{-1} can be assigned to hydrogen-bonded water molecules that are present in the protein film. Apparently, certain parts of the molecule pertain to their hydration shell. The features below 1200 cm^{-1} probably originate from skeletal modes of the numerous bonds inside the protein. The fact that the increase in intensity is not extremely large could be interpreted to indicate that the amount of linked L1 is small. This is corroborated by the QCM data. The most notable differences between the NTA film and the NTA-L1 film are in the OH stretching region, the amide region, and the

skeletal region of the IR spectrum. To determine whether these changes have anything to do with surface-specific complexation, we have performed VSFG spectroscopy, which is discussed in the next section.

Surface Binding of L1 Studied with VSFG. To get a better idea of the nature of the interaction, we have taken VSFG spectra in various spectral windows. The VSFG signal is generated by the simultaneous interaction of an infrared (IR) and a visible (VIS) photon in the interfacial region. Simultaneous interaction is achieved only when the IR dipole moment and Raman transition moment of a molecule are both nonzero. This can occur (in cases where the electric dipole transition moment is the leading-order term, which is true in almost all cases for VSFG⁴²) only in regions where inversion symmetry is absent.

For the case of a molecular film on a substrate, this means that two different electric field components can arise. The first one is a nonresonant signal from the Ag(111) surface. The second signal is resonant and originates from all parts of NTA and the NTA-L1 complex that have a certain preferential order. Parts of the complex that do not have any order on the molecular length scale are amorphous and do not generate a sum frequency (SF) field that is distinguishable from the nonresonant field generated by the Ag film. Both electric-field components interfere and give rise to the following VSFG intensity:^{22,24,43}

$$I_{\text{VSFG}}(\omega) \propto \left| E_{\text{IR}}(\omega) \sum_n \int_{-\infty}^{\infty} (\chi_n^{(2)}(\omega') + \chi_{\text{NR}}^{(2)}) E_{\text{VIS}}(\omega' - \omega) d\omega' \right|^2, \\ \chi_{\text{NR}}^{(2)} = A_{\text{NR}} e^{i\Delta\phi}, \quad \chi_n^{(2)}(\omega) = \frac{N_s A_n}{(\omega - \omega_{0n}) + i\Gamma_n} \quad (1)$$

This signal consists of a nonresonant (frequency-independent) contribution and n resonant electrical-field contributions. The resonant contributions are described as damped exponentially decaying oscillators with (relative) amplitude A_n , resonance frequency ω_{0n} , and damping constant Γ_n . N_s is the density of surface molecules. The frequency-independent nonresonant response has amplitude A_{NR} and follows the shape of the femtosecond infrared pulse, which is a broadband signal in the frequency domain. $\Delta\phi$ represents the phase difference between the resonant and nonresonant fields.

Figure 4 shows VSFG spectra taken in the C-H stretching region for the NTA film and the NTA-L1 film. The spectra were recorded in ppp polarization (i.e., all beams are polarized parallel to the plane of incidence). Although the RAIRS spectra do not display a change in this spectral region, the difference in the VSFG

(41) Colthup, N. B.; Daly, L. H.; Wiberley, S. E. *Introduction to Infrared and Raman Spectroscopy*; Academic Press: New York, 1975.

(42) Held, H.; Lvovsky, A. I.; Wei, X.; Shen, Y. R. *Phys. Rev. B* **2002**, *66*, 1–7.
(43) Guyot-Sionnest, P.; Hunt, J. H.; Shen, Y. R. *Phys. Rev. Lett.* **1987**, *59*, 1597–1600.

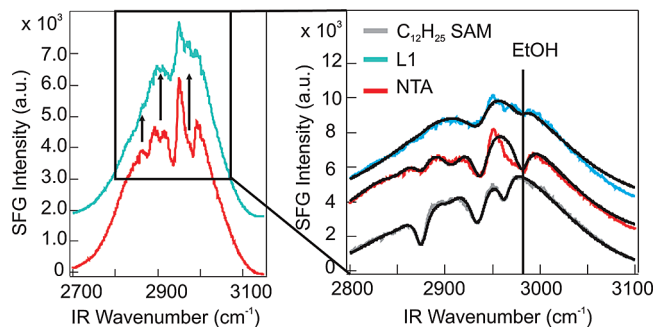


Figure 4. Broadband vibrational sum frequency generation spectra in the C–H stretching region of self-assembled monolayers on (111)-oriented silver linked with L1 protein. (Left) Spectra of silver films with NTA (bottom) and NTA with L1 protein (top). The arrows indicate a significant reduction in the methyl stretching mode intensity, which indicates that ethanol has been replaced by His-tagged L1. The spectra are raw data. (Right) Close-up of the spectral region around the vibrational resonances. The bottom spectrum is from a self-assembled monolayer of $C_{12}H_{25}SH$ on Ag(111). The fits (black lines) were made with eq 1, and the ethanol signature is indicated in the graph. The spectra are offset for clarity.

spectra is remarkable. The left panel displays the raw data, and the right panel displays close-up fits of the spectra. The spectra were fit using for the IR and VIS electric field envelopes Gaussian pulse shapes obtained from fitting an SFG spectrum from a clean metal substrate (for IR) or measuring the pulse-shaped spectrum with a spectrometer and an I-CCD camera (for the VIS pulse). Also shown is a spectrum of a self-assembled monolayer of $C_{12}H_{25}SH$ prepared on Ag(111) (C12-SAM). The C12-SAM spectrum is taken as a reference so that it is possible to identify the methyl and methylene stretching modes unambiguously. It displays the characteristic resonances of the symmetric methyl stretching mode (at 2875 cm^{-1}), the antisymmetric methyl stretching mode (at 2963 cm^{-1}), the Fermi resonance of the methyl stretching mode (at 2935 cm^{-1}), and two weak methylene stretching modes (at 2848 and 2904 cm^{-1}). These peaks correspond well with earlier measurements on SAMs.^{44–46} The relative phase between the resonant and nonresonant response ($\Delta\phi$) was determined to be 90° . To make the fits to the other two films without knowing which L1 groups appear in the spectrum, we started with the same phase and frequencies because they represent the values of measured methyl and methylene vibrational modes that are originating from methyl and methylene groups that are bound to a Ag surface.

For the NTA film, we find that the phase difference can be kept constant and that the peaks at 2875 and 2935 cm^{-1} (which is shifted to 2937 cm^{-1}) decrease somewhat in intensity. Because NTA has a more bulky chemical structure than C12-alkanethiol, the surface density of NTA can be expected to be lower, which would explain the difference in intensity. Interestingly, a new peak appears at 2982 cm^{-1} . This is a very high frequency for a methyl group and is indeed absent in the C12-SAM spectrum. Also, the chemical structure of NTA does not contain any methyl groups. Ethanol, however, does. It was recently reported that both the infrared spectrum of gas-phase ethanol⁴⁷ and the vibrational sum

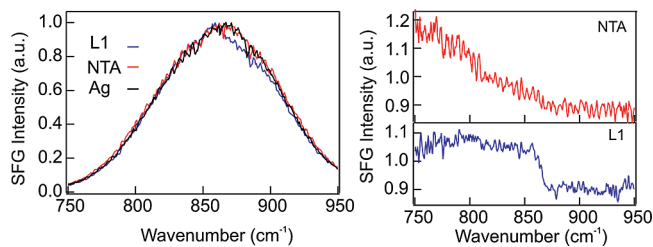


Figure 5. (Left) Broadband vibrational sum frequency generation spectra in the C–C stretching region of a Ag(111) surface, NTA films on top of Ag(111), and L1–NTA on top of Ag(111). (Right) NTA (top) and NTA–L1 (bottom) spectra divided by the spectrum of the bare silver surface. It can be seen that only in the case of L1 there is a discontinuity that points toward a possible resonance contribution of L1 at 866 cm^{-1} .

frequency generation spectrum of the air/ethanol interface⁴⁸ display a peak at 2983 cm^{-1} . This peak was assigned to the asymmetric methyl stretch mode of isolated gas-phase-like ethanol on the surface of liquid ethanol. This makes it very likely that the NTA surface contains ethanol. Considering the chemical structure, it is likely that the ethanol binds to the carboxylate groups of NTA and thereby stabilizes the complex.

Subsequent binding of His-tagged L1 to the NTA complex should then give rise to a disappearing ethanol signature in the SFG spectrum. This can be seen in the upper trace of Figure 4b, where the peak at 2982 cm^{-1} has diminished and the only remaining significant mode is the Fermi resonance at 2937 cm^{-1} , which appears with a relative phase of 43° with respect to the nonresonant background. The fact that the VSFG spectrum of NTA–L1 does not display any more structure indicates that the protein is amorphous. The difference in phase seems to suggest that some part of the protein contributes to the nonresonant background. This is not surprising because the protein could not be characterized by X-ray diffraction.

Because the RARS data of the L1 films in Figure 2 show clear vibrational features in the spectral regions of $1600\text{--}1800\text{ cm}^{-1}$ and $800\text{--}1000\text{ cm}^{-1}$, we have (unsuccessfully) performed SFG spectroscopy also in these regions. The RARS spectra do show an amide peak, which corroborates the XRD data that shows that the immunoglobulin and fibronectin-like III domains in the extracellular domain of L1 contain α helices and β sheets. In the amide region of the VSFG spectrum, we were not able to distinguish any surface vibrational resonances, which means that the α -helices and β -sheets in the protein do not form any preferentially ordered structures. Considering that they have a clear signature in the RARS spectrum and that even weakly oriented chemical groups can be observed with VSFG, it seems that the amide groups do not play a role in the interaction with the surface. In the spectral region from 800 to 1000 cm^{-1} , we find a minor but reproducible difference in spectral response between the NTA–L1 film and the NTA films. The result is shown in Figure 5. In the left panel, the spectra obtained in ppp polarization are displayed. The right panel shows the ratio of the spectrum of the NTA film with the spectrum of the Ag surface and the ratio of the spectrum of the L1–NTA film with the spectrum of the Ag surface. It can be seen that at 866 cm^{-1} a small resonance appears. A reasonable assignment for this band could be substituted aromatic rings, which are present in proteins and may have the capability to form small ordered domains, detectable by VSFG. In the primary sequence of the full-length clone of human L1,

(48) Gan, W.; Zhang, Z.; Feng, R.; Wang, H. F. *Chem. Phys. Lett.* **2006**, *423*, 261–265.

(44) Bain, C. D.; Davies, P. B.; Ong, T. H.; Ward, R. N.; Brown, M. A. *Langmuir* **1991**, *7*, 1563–1566.

(45) Yeganeh, M. S.; Dougal, S. M.; Polizzotti, R. S.; Rabinowitz, P. *Phys. Rev. Lett.* **1995**, *74*, 1811–1814.

(46) Buck, M.; Himmelhaus, M. *J. Vac. Sci. Technol., A* **2001**, *19*, 2717–2736.

(47) Yu, Y.; Lin, K.; Zhou, X.; Wang, H.; Liu, S.; Ma, X. *J. Phys. Chem. C* **2007**, *111*, 8971–8978.

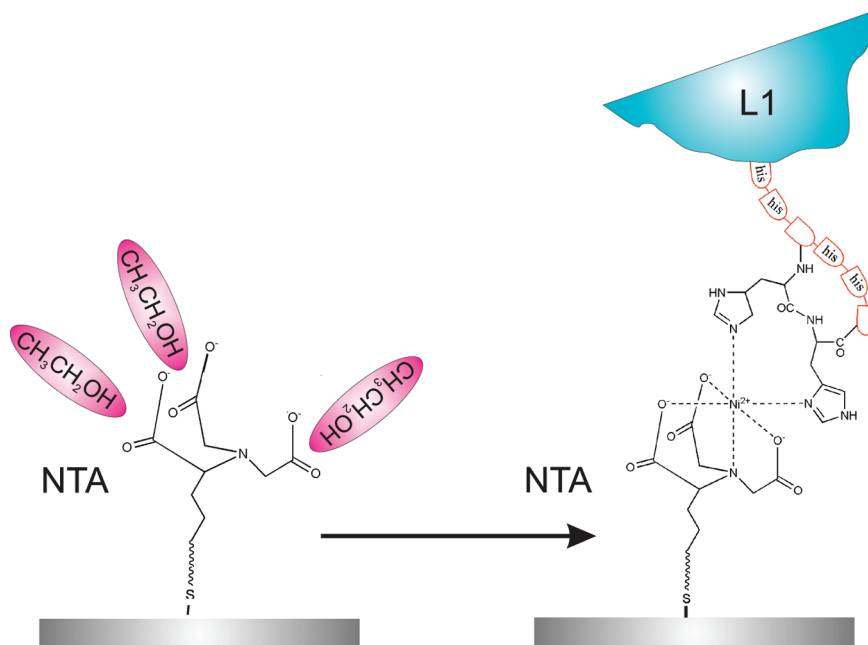


Figure 6. Illustration of the chemical structure of the surface NTA complex before (left) and after the binding (right) of L1 to the NTA complex. Upon binding, the ethanol molecules that cover the carboxylate groups are displaced by the protein.

around 9% of the amino acids contain substituted aromatic rings (tryptophan, tyrosin, and phenyl-alanine).⁴⁹ Aromatic amino acids located in the highly structured extracellular immunoglobulin domains of L1 might be responsible for that signal. Because we conducted measurements in 100% humid nitrogen flow, we have not taken any VSFG spectra above 3000 cm^{-1} .

It should be noted that our measurements were conducted in humid air and not in water, which means that some part of the proteins' organized structure (if present in the water phase) might be lost in air. For the samples investigated in this study, however, we have observed biological activity before and after our VSFG measurements by performing cell adhesion experiments with a static cell adhesion assay (as described in ref 8). Also, a clear water signature in the RAIRS measurements was observed. This would mean that even though the spatial structure of the protein might be perturbed by the absence of liquid water, this structural change is not irreversible so that a fair portion of the biologically indicated directionality is preserved.

We estimate that the required surface area per molecule is on the order of ~ 10 to perhaps 100 nm^2 (see, for example, refs 24 and 50) in order to be detected with VSFG. The absence of strong VSFG features indicates that the surface structure does not consist of well-organized repeated building blocks or that there is not a high enough surface density or a combination of both. The strength of the RAIRS signal suggests that it is not likely to be only a density issue. Cell activity means that there is interaction between proteins in or on the cell and the extracellular domains of the proteins on the surface. It is not known how many active surface proteins are needed to induce cellular activity. The cells in the picture in Figure 1c have a typical area of $\sim 300\text{ }\mu\text{m}^2$. If such a cell requires only a few active proteins, then it is not really surprising that the VSFG measurements do not display any clear features that can be linked to the protein. One way of observing a stronger VSFG signal would be to include the cells in the

experiment.³⁶ This might result in clear features, but it might not be clear what they mean.

The biological model that initiated this study assumes a certain amount of order and directionality on the substrate. We have shown that this does not mean, however, that the surface structure should consist of well-organized repeating building blocks that can be detected in a surface science experiment. Thus, what is referred to as order and directionality in a biological context does not necessarily appear to be ordered and directional in a surface science experiment. We believe that this article demonstrates some of the possibilities and constraints that can be a result of combining surface science methods with biological experiments. Although our work offers a start, it is clear that much more work is required to achieve a complete molecular understanding of cellular–biological functionality on surfaces.

Conclusions

To summarize, we have investigated the interaction of *N*-cadherin and L1 with self-assembled NTA films using a combination of methods that detect surface viscosity and mass change (QCM), the change in the average chemical film structure (RAIRS), and the change in chemical groups that have a preferential order (VSFG). These methods are complementary and allow one to probe noninvasively the average structural changes as well as the structural changes in the surface binding centers. The measurements show that NTA-SAMs are formed but with less preferential density than a grown *n*-alkanethiol C12-SAM. Subsequent addition of His-tagged *N*-cadherin and his-tagged L1 in quantities used to obtain biological functionality results in a small amount of protein bound to the surface. Because the amount of adsorbed L1 is greater than the amount of adsorbed *n*-cadherin, we have continued the spectroscopic investigation only of trans-membrane protein L1. We found that it interacts by replacing capping ethanol molecules, which are most likely linked to the carboxylate groups of the NTA complex (Figure 6). From the RAIRS data, we find that L1 links to the NTA film, whereby L1 pertains to its hydration shell. This could

(49) <http://www.ncbi.nlm.nih.gov/entrez/viewer.fcgi?db=protein&id=187951475>.

(50) Roke, S.; Buitenhuis, J.; van Miltenburg, J. C.; Bonn, M.; van Blaaderen, A. *J. Phys.: Condens. Matter* **2005**, *17*, S3469–S3479.

be the most important factor for the observed biological functionality, which is still present after exposure to air. Although the RAIRS spectrum is rich in features in the amide and fingerprint regions, we do not find much evidence of that in the VSFG spectra, which indicates that the protein is amorphous and that the present α helices and β sheets do not play a (directional) role in the protein-surface interaction.

Experimental Section

Au(111)- and Ag(111)-oriented surfaces on mica were obtained from PVD-Coatings (Heidelberg, Germany). The substrates were functionalized using mono NTA-thiols (Prochimia) (an alkanethiol with a triethylene glycol-linked nitrilotriacetic acid head-group).^{9,51,52} A stock solution of NTA was diluted to a 1 mM working solution in ethanol (p.a., Merck) and incubated for 4 h at room temperature. After washing with hepes-buffered saline solution (HBSS), a solution of 10 mM NiCl₂ in HBSS was applied to the surfaces. After two additional washing steps, His-tagged extracellular domains of L1⁵³ (L1 aa 1-1120, obtained from R & D Systems with a mass of 114 kDa) and N-cadherin (obtained through the procedure described in ref 8 with a mass of 210 kDa)⁵⁴ were immobilized onto the NTA-Ni²⁺ complexes on the substrates. Protein solutions in phosphate-buffered saline (PBS) solution (Gibco) with a concentration of 50 μ g/mL were incubated overnight at 4 °C. Finally, samples were washed three times with PBS and stored in PBS at 4 °C until measurements were conducted.

Phase-contrast microscopy images were obtained with a Zeiss Axiovert microscope using a 20 \times objective.

Quartz crystal microbalance (QCM) measurements were performed using the Q SENSE E4 system equipped with standard flow module QFM 401 (Q-SENSE AB, Gothenburg, Sweden) as described in detail elsewhere.^{16,17} The mass adsorption data was

acquired at 23 °C with gold-coated QCM sensors with a fundamental resonance frequency of 4.95 ± 0.02 MHz and an active sensor area of 78 mm² (QSX 301- Standard Gold; Q-SENSE AB, Gothenburg, Sweden). Briefly, the QCM response is continuously recorded as a function of the frequency change with respect to the resonance frequency of the quartz crystal with a time resolution of better than 1 s. The response is sensitive to any mass or viscosity change in the sensor crystal.^{55,56} The sample solution was flushed through to the measurement chamber at a flow rate of 100 μ L using a peristaltic pump (ISM935C, Ismatec, Zurich, Switzerland), using a flow rate of 50 μ L/min. To switch between sample liquids, the flow was interrupted for a few seconds without disturbing the measured signals. A commercial software program (Q-Tools, Q-Sense AB, Gothenburg, Sweden) was used to monitor the frequency change.

RAIRS experiments were conducted by pressing a functionalized silver film onto a ZnSe ATR prism of a Bruker Vertex 70 IR spectrometer. Spectra were recorded with an acquisition time of 256 s. The resolution was 4 cm⁻¹. A clean silver substrate was used as a background.

The broadband VSFG experiments were conducted using a 1 kHz 70 fs high-power Ti:sapphire laser system, described in detail in ref 57. The p-polarized VIS pulses had an energy of 3 μ J per pulse and were centered at 810 nm with a typical bandwidth of 5 cm⁻¹. The IR laser beam was tuned to different wavelengths (i.e., centered at 2920 cm⁻¹ to probe C-H stretching vibrations, 1650 cm⁻¹ for the amide-I and amide-II regions, and from 700 to 1000 cm⁻¹ for C-C vibrations). Frequency-resolved signal collection was done with a spectrometer (Shamrock, Andor Technology, Ireland) in combination with an intensified CCD camera (I-Star, Andor Technology, Ireland). The typical acquisition time was 200 s per spectrum. Samples were rinsed with distilled water and dried in a nitrogen flow before being mounted into the VSFG setup and were kept in a 100% humid nitrogen flow during the experiments.

Acknowledgment. This work is part of the research program of the Max-Planck Society. We thank J. P. Spatz for providing access to the microscope and QCM and E. Weiss and G. M. Whitesides for gold and silver template surfaces as well as fruitful discussions.

(57) Sugiharto, A. B.; Johnson, C. M.; de Aguiar, H. B.; Aloatti, L.; Roke, S. *Appl. Phys. B* **2008**, *91*, 315–318.

(51) Sigal, G. B.; Bamdad, C.; Barberis, A.; Strominger, J.; Whitesides, G. M. *Anal. Chem.* **1996**, *68*, 490–497.

(52) Cheng, F.; Gamble, L. J.; Castner, D. G. *Anal. Chem.* **2008**, *80*, 2564–2573.

(53) Moos, M.; Tacke, R.; Scherer, H.; Teplow, D.; Früh, K.; Schachner, M. *Nature* **1988**, *334*, 701–703.

(54) Shirayoshi, Y.; Hata, K.; Hosoda, M.; Tsunasawa, S.; Sakiyama, F.; Takeichi, M. *EMBO J.* **1986**, *5*, 2485–2488.

(55) Suaerbrey, G. Z. *Phys.* **1959**, *155*, 206–222.

(56) Plunkett, M. A.; Claesson, P. M.; Ernstsson, M.; Rutland, M. W. *Langmuir* **2003**, *19*, 4673–4681.